AMERICAN SOCIETY FOR MICROBIOLOGY | mBio®

RESEARCH ARTICLE

Deep-Sea *In Situ* Insights into the Formation of Zero-Valent Sulfur Driven by a Bacterial Thiosulfate Oxidation Pathway

Ruining Cai,[a,b,c,e] Wanying He,[c,d,e] Rui Liu,[a,b,e] Jing Zhang,[a,b,c,e] Xin Zhang,[d,e] Chaomin Sun[a,b,e]

[a]CAS Key Laboratory of Experimental Marine Biology & Center of Deep Sea Research, Institute of Oceanology, Chinese Academy of Sciences, Qingdao, China
[b]Laboratory for Marine Biology and Biotechnology, Qingdao National Laboratory for Marine Science and Technology, Qingdao, China
[c]College of Earth Science, University of Chinese Academy of Sciences, Beijing, China
[d]CAS Key Laboratory of Marine Geology and Environment & Center of Deep Sea Research, Institute of Oceanology, Chinese Academy of Sciences, Qingdao, China
[e]Center of Ocean Mega-Science, Chinese Academy of Sciences, Qingdao, China

ABSTRACT Zero-valent sulfur (ZVS) distributes widely in the deep-sea cold seep, which is an important immediate in the sulfur cycle of cold seep. In our previous work, we described a novel thiosulfate oxidation pathway determined by thiosulfate dehydrogenase (TsdA) and thiosulfohydrolase (SoxB) mediating the conversion of thiosulfate to ZVS in the deep-sea cold seep bacterium *Erythrobacter flavus* 21-3. However, the occurrence and ecological role of this pathway in the deep-sea cold seep were obscure. Here, we cultured *E. flavus* 21-3 in the deep-sea cold seep for 10 days and demonstrated its capability of forming ZVS in the *in situ* field. Based on proteomic, stoichiometric analyses and microscopic observation, we found that this thiosulfate oxidation pathway benefited *E. flavus* 21-3 to adapt the cold seep conditions. Notably, ~25% metagenomes assembled genomes derived from the shallow sediments of cold seeps contained both *tsdA* and *soxB*, where presented abundant sulfur metabolism-related genes and active sulfur cycle. Our results suggested that the thiosulfate oxidation pathway determined by TsdA and SoxB existed across many bacteria inhabiting in the cold seep and frequently used by microbes to take part in the active cold seep biogeochemical sulfur cycle.

IMPORTANCE The contribution of microbes to the deep-sea cold seep sulfur cycle has received considerable attention in recent years. In the previous study, we isolated *E. flavus* 21-3 from deep-sea cold seep sediments and described a novel thiosulfate oxidation pathway in the laboratorial condition. It provided a new clue about the formation of ZVS in the cold seep. However, because of huge differences between laboratory and *in situ* environment, whether bacteria perform the same thiosulfate oxidation pathway in the deep-sea cold seep should be further confirmed. In this work, we verified that *E. flavus* 21-3 formed ZVS using this pathway in deep-sea cold seep through *in situ* cultivation, which confirmed the importance of this thiosulfate oxidation pathway and provided an *in situ* approach to study the real metabolism of deep-sea microorganisms.

KEYWORDS zero-valent sulfur, deep sea, cold seep, *in situ*, thiosulfate oxidation

Zero-valent sulfur (ZVS) distributes widely in the deep-sea cold seep, which is an important immediate in the active sulfur cycle of the cold seep (1–3). ZVS production for bacteria is a strategy to conserve energy (4). Thiosulfate is regarded as a key substance in the sulfur cycle of marine sediments, which is a common substrate oxidized by almost all sulfur bacteria (5). Therefore, microbial thiosulfate oxidation pathways provide a new clue to the ZVS formation in the deep-sea cold seep (6, 7).

The conversion of thiosulfate to ZVS can be completed by microbes through three pathways at least. For the typical sulfur-oxidizing enzyme (Sox) system, the multienzyme

Invited Editor Joel E. Kostka, Georgia Institute of Technology
Editor Xiaorong Lin, University of Georgia

Address correspondence to Chaomin Sun, sunchaomin@qdio.ac.cn.
The authors declare no conflict of interest.
Received 17 January 2022
Accepted 30 June 2022
Published 19 July 2022

complex consisting of SoxXA, SoxYZ, SoxB, and SoxCD has the capacity of oxidizing sulfide, ZVS, sulfite, and thiosulfate to sulfate as the final product (8, 9). This pathway operates in photo- and chemolithotrophic *Alphaproteobacteria* (9, 10). However, for organisms deficient in SoxCD complex, the sulfur atom of sulfane bound to SoxY cannot be oxidized further, whereas it is transferred to produce periplasmic or extracellular ZVS (11–14). Exceptionally, *Thiomicrospira thermophila* could produce extracellular ZVS at low pH though *soxCD* genes (15). Tetrathionate intermediate (S_4I) pathway is also a thiosulfate oxidation pathway distributing in *Proteobacteria* including *Acidithiobacillia*, *Alpha-*, *Beta-*, *and Gamma proteobacteria* (16–19). This pathway was made up of thiosulfate: quinol oxidoreductase (TQO or DoxDA) and tetrathionate hydrolase (TetH or TTH) (20). TQO oxidizes thiosulfate to tetrathionate while TTH hydrolyzes tetrathionate to thiosulfate, ZVS and sulfate as final products (19, 21).

In our recent work, a novel thiosulfate oxidation pathway discovered in the deep-sea cold seep bacterium *Erythrobacter flavus* 21-3 was described, which provided a new clue about the formation of ZVS (6). Thiosulfate dehydrogenase (TsdA) and thiosulfohydrolase (SoxB) were identified to play key roles in the conversion of thiosulfate to ZVS. In this novel pathway, TsdA converted thiosulfate to tetrathionate, and SoxB liberated sulfone from tetrathionate to form ZVS. However, whether this novel thiosulfate oxidation pathway occurs in the deep-sea cold seep remains obscure. Actually, key genes involved in this novel pathway were found in many sulfur oxidizing bacteria living in the deep-sea cold seep (6, 22). Therefore, microbes using this pathway were proposed to be an important part in the sulfur cycle of deep-sea cold seeps (6). However, because of huge differences between laboratory and *in situ* environment, whether bacteria perform the same thiosulfate oxidation pathway in the deep-sea condition as they were cultivated in the laboratory should be further confirmed.

To investigate whether *E. flavus* 21-3 produces ZVS in the deep-sea cold seep using the same pathway, we *in situ* incubated *E. flavus* 21-3 wild type (WT) and mutants with deletion of key gene(s) determining the formation of ZVS in the deep-sea cold seep located in the South China Sea for 10 days, and we found *E. flavus* 21-3 could produce ZVS in the deep-sea cold seep through the same thiosulfate oxidation pathway. Based on proteomic, stoichiometric, and microscopic results, distinctions between *E. flavus* 21-3 cultivated in the deep-sea cold seep and laboratory with/without activating the thiosulfate oxidation pathway were compared. Moreover, sulfur metabolism-related genes in the deep-sea cold seep sediments and broad distribution of bacteria potentially used this pathway were investigated and discussed.

RESULTS AND DISCUSSION

***E. flavus* 21-3 is capable of producing ZVS in the deep-sea cold seep.** In our recent work (6), in the laboratorial condition, we isolated a bacterium named *E. flavus* 21-3 from deep-sea cold seep sediments and identified a novel thiosulfate oxidation pathway. It is able to convert thiosulfate to ZVS through thiosulfate dehydrogenase (TsdA) and thiosulfohydrolase (SoxB). Given the special environmental condition of deep-sea cold seep, we sought to ask whether *E. flavus* 21-3 produces ZVS in the cold seep through this pathway. To this end, *E. flavus* 21-3 WT and mutants Δ*soxB* and Δ*tsdA* were *in situ* incubated for 10 days in the cold seep of the South China Sea where we isolated *E. flavus* 21-3 (Fig. S1 in the supplemental material). To check whether general sulfur-containing substrates involved in sulfur metabolism existed in the study site, the concentrations of sulfide, sulfite, sulfate and thiosulfate in sediments and seawater were measured (Table S1). Among them, thiosulfate, which was regarded as the main substrate driving the formation of ZVS in *E. flavus* 21-3, was determined as 137.76 μM in sediments. It provided basis for *E. flavus* 21-3 to perform thiosulfate oxidation in the deep-sea cold seep.

To confirm whether *E. flavus* 21-3 WT and mutants Δ*soxB* and Δ*tsdA* produced ZVS in the deep-sea cold seep, electron microscopic observation and Roman Spectra analyses

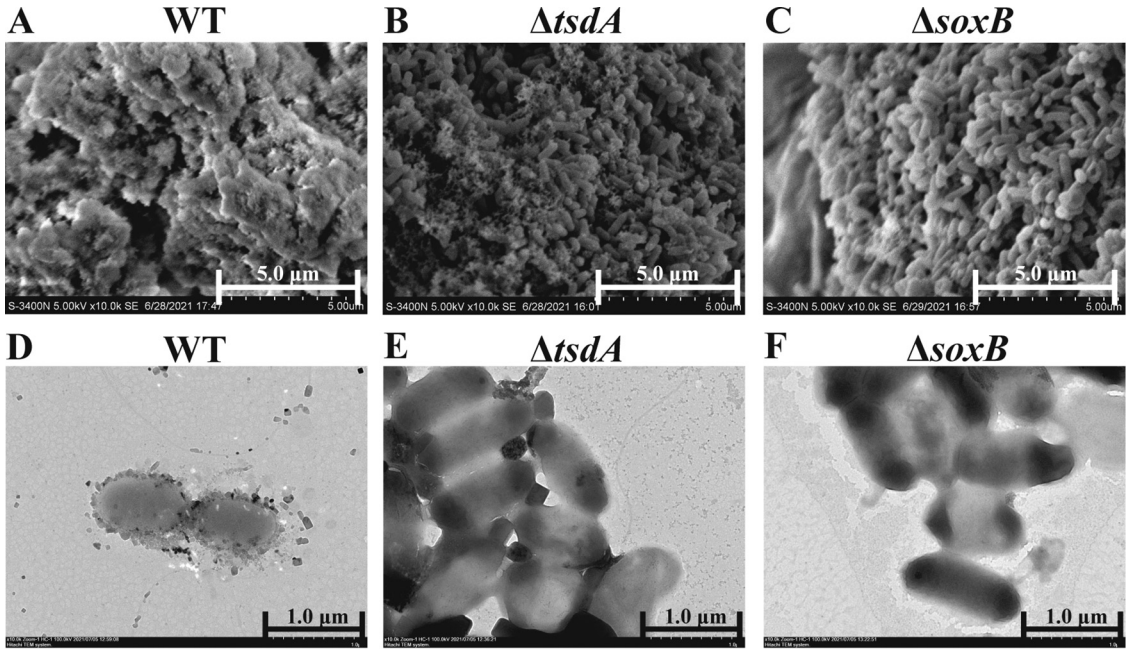

FIG 1 The electron microscopic images of *E. flavus* 21-3 wild type and mutants Δ*tsdA* and Δ*soxB* after 10-day *in situ* cultivation. Scanning electron microscopic (SEM) images of *E. flavus* 21-3 wild type (A) and mutants Δ*tsdA* (B) and Δ*soxB* (C) after 10-day *in situ* cultivation. Transmission electron microscopic (TEM) images of *E. flavus* 21-3 wild type (D) and mutants Δ*tsdA* (E) and Δ*soxB* (F) after 10-day *in situ* cultivation.

were performed. Scanning electron microscopy (SEM) results showed that the WT cells were completely embedded in ample fibrous substances (Fig. 1A). However, less fibrous substances appeared on the surface of the mutant Δ*tsdA* (Fig. 1B), and were even totally absent on the surface of the mutant Δ*soxB* (Fig. 1C). Consistently, TEM results showed that many particles (~100-200 nm) attached to the surfaces of WT (Fig. 1D and Fig. S2A in the supplemental material) and the mutant Δ*tsdA* (Fig. 1E and Fig. S2B) but not to the surface of the mutant Δ*soxB* (Fig. 1F and Fig. S2C). The attachments presented on the surfaces of WT and the mutant Δ*tsdA* were further identified as sulfur-containing substances by EDS (Fig. 2A and B). Consistently, sulfur element couldn't be detected on the surface of the mutant Δ*soxB* (Fig. 2C). To verify whether these substances attached to the cells included ZVS, the attachments presented on the surface of deep-sea *in situ* cultured cells were extracted and checked by Raman Spectra. The strong Raman peak at ~475 Δcm^{-1} indicated S_8 (a form of ZVS) was produced by the WT and the mutant Δ*tsdA* in the cold seep (Fig. 2D). Consistently, the highest concentration of ZVS was detected in WT, much less in the mutant Δ*tsdA*, and almost none in the mutant Δ*soxB* (Fig. 2E). Notably, we observed the formation of S_8 in the deep-sea cold seep where strain 21-3 was isolated (3), suggesting deep-sea microorganisms (e.g., strain 21-3) have potential contribution to the formation of ZVS in deep-sea cold seeps. These results clearly showed that *E. flavus* 21-3 was able to produce ZVS in the cold seep and *tsdA* and *soxB* were the key genes in determining the formation of ZVS under both *in situ* and laboratorial conditions (6).

Besides, membrane vesicle-like structures were also observed on the surfaces of the WT (Fig. S2D) and the mutant Δ*tsdA* (Fig. S2E) but not on the surface of the mutant Δ*soxB* (Fig. S2F) based on the observation of ultrathin sections. Similar structure was observed and regarded as part of the detoxification mechanism in archaea and bacteria (23–25). For example, *Thermococcus prieurii* used membrane vesicles to export intracellular ZVS for avoiding the toxicity of sulfur in high concentration (23); *Allochromatium vinosum*, whose membrane vesicles were observed ever, could take up ZVS as electron donor (26, 27); *Chlorobaculum tepidum* which producing extracellular ZVS through same vesicles, could also transiently attach to sulfur globules for fuel subsequent growth (28, 29).

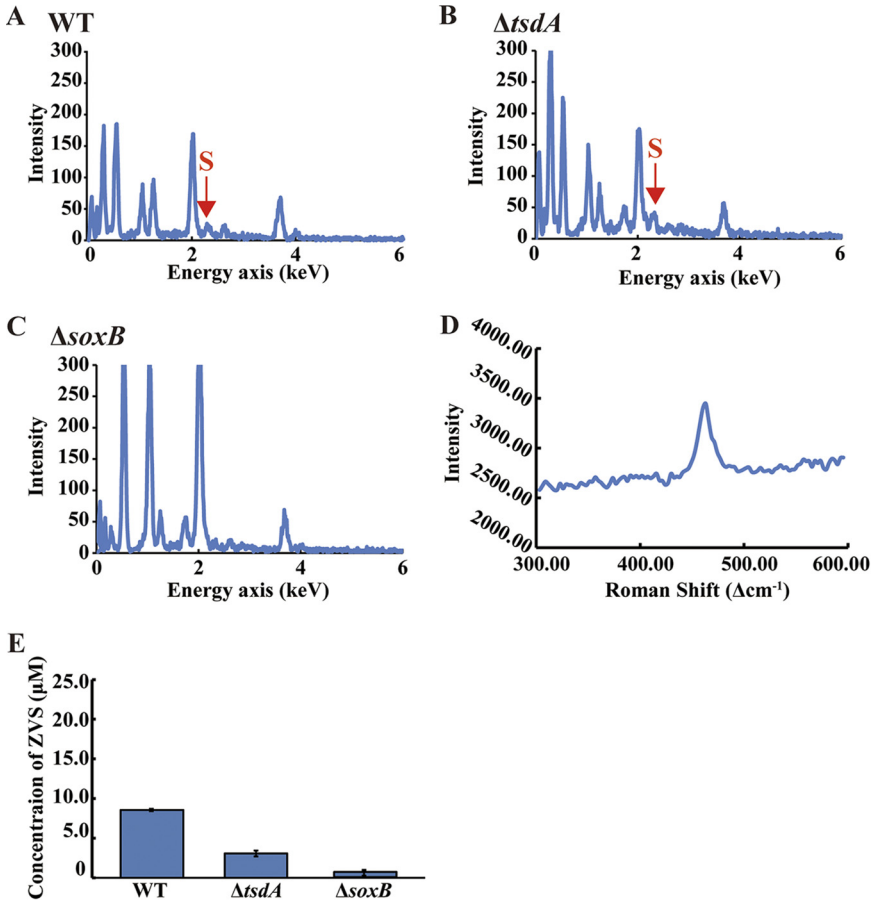

FIG 2 Verification of zero-valent sulfur (ZVS) formed by *E. flavus* 21-3 and mutants Δ*tsdA* and Δ*soxB* that cultured in the deep-sea cold seep. Energy dispersive spectrum analysis of substances formed in the surfaces of *E. flavus* 21-3 wild type (A) and mutants Δ*tsdA* (B) and Δ*soxB* (C). (D) The Raman peak at ~475 Δcm^{-1} of standard S_8. (E) Measurement of the concentration of ZVS formed by *E. flavus* 21-3 wild type and mutants Δ*tsdA* and Δ*soxB* that cultured in the deep sea for 10 days.

Therefore, the membrane vesicles were proposed to be essential for transportation, storage and utilization of ZVS for microorganisms including *E. flavus* 21-3. It needs further verification in the future.

Biological functions of ZVS formation for *E. flavus* 21-3. Next, we sought to ask what biological functions of ZVS formation for *E. flavus* 21-3 in the deep-sea cold seep. For this purpose, proteomic assays of *in situ* cultured *E. flavus* 21-3 WT and mutants (Δ*tsdA* and Δ*soxB*) were performed. Compared with proteins expression of the WT, 126 of 988 and 200 of 850 proteins were significantly down-regulated in the mutants Δ*tsdA* and Δ*soxB*, respectively ($P < 0.05$). The abundance-reduced proteins in both mutants Δ*tsdA* and Δ*soxB* fell into the COG categories of energy production and conversion (Fig. 3A). Furthermore, analyses based on KEGG database showed most proteins associated with the glycolysis, gluconeogenesis and TCA cycle were down-regulated in the mutants Δ*tsdA* and Δ*soxB* (Fig. 3B and C). Besides, compared to the mutant Δ*tsdA* which could produce ZVS in the cold seep, most proteins in the mutant Δ*soxB* which couldn't produce ZVS were down-regulated (Fig. 3). According to these results, we speculate that ZVS should be important to the growth, energy conservation of *in situ* incubated *E. flavus* 21-3 in the cold seep. *E. flavus* 21-3 was thus proposed to grow better in the presence of ZVS.

To verify the deduction above, ZVS produced by *E. flavus* 21-3 was purified and added to the ASW as the sole electron donor. Continuous measurements of the biomass showed that ZVS promoted the growth of *E. flavus* 21-3 (Fig. 4A). Accordingly,

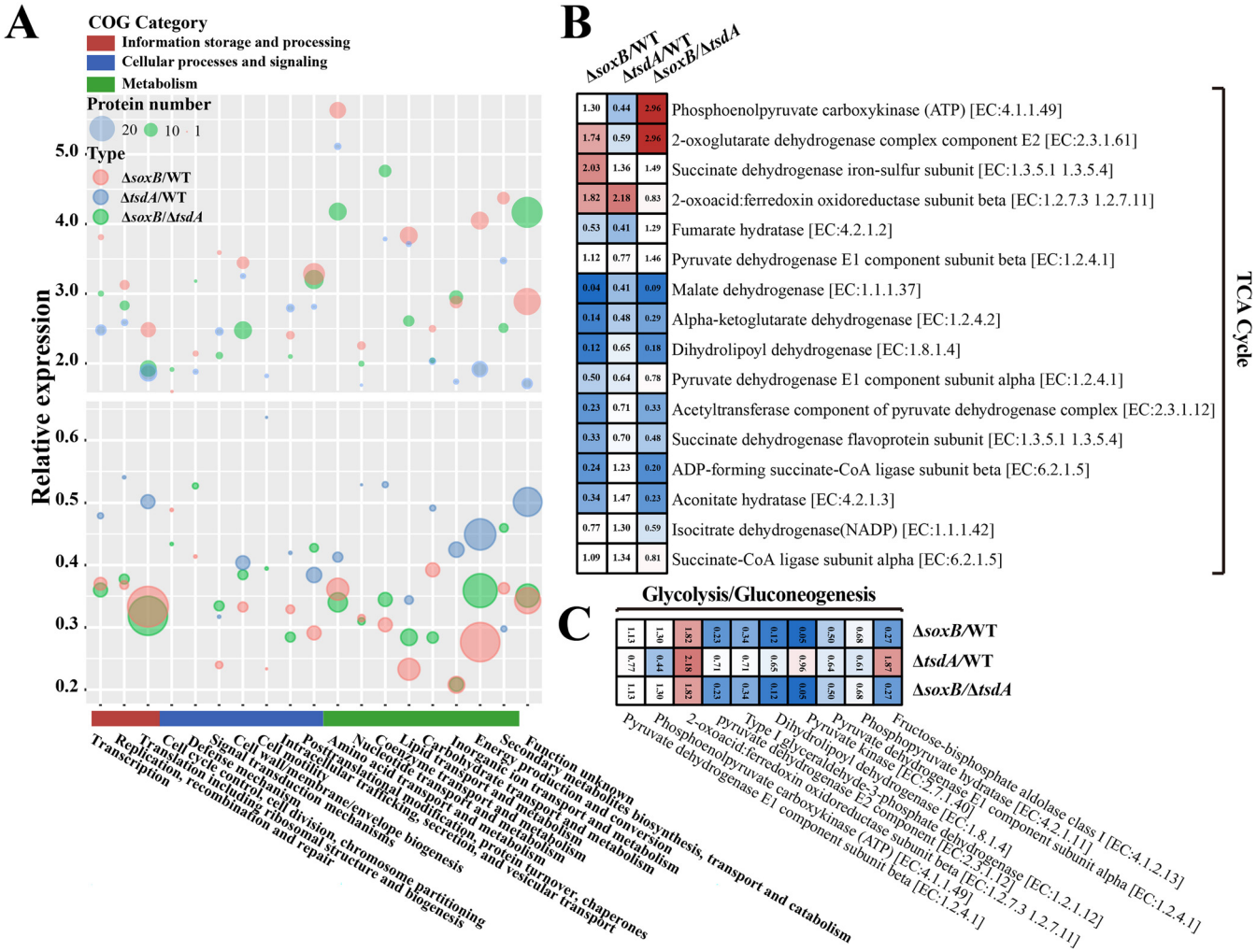

FIG 3 Comparative proteomic analysis of *E. flavus* 21-3 wild type and mutants Δ*tsdA* and Δ*soxB* that cultured in the deep-sea colds seep for 10 days. (A) Comparative analysis of the number and relative expression level of proteins in *E. flavus* 21-3 wild type and mutants Δ*tsdA* and Δ*soxB* in different COG categories. (B) Heatmap analysis of differentially expressed proteins in TCA cycle of *E. flavus* 21-3 wild type and mutants Δ*tsdA* and Δ*soxB*. (C) Heatmap analysis of differentially expressed proteins in glycolysis and gluconeogenesis of *E. flavus* 21-3 wild type and mutants Δ*tsdA* and Δ*soxB*.

after 6-day cultivation, the concentration of remaining ZVS significantly decreased, strongly suggesting ZVS was consumed by *E. flavus* 21-3 (Fig. 4B). To better characterize the growth of *E. flavus* 21-3 in the medium supplemented without or with ZVS, we further checked the morphology of *E. flavus* 21-3 that cultured in the above conditions using TEM. The results clearly showed that many extra particles (~200 nm) attached to surfaces of bacterial cells that cultured with supplemental ZVS (Fig. 4C and D), while none of above particles was observed around bacterial cells that cultured without ZVS (Fig. 4E and F). And these particles around bacterial cells were further identified as element sulfur through the EDS analysis (Fig. 4G and H). Of note, the amount of ZVS attached to bacterial cells showed an evident decrease trend along with the incubation time from 7 days (Fig. S3A and S3B) to 14 days (Fig. S3C and S3D), strongly suggesting *E. flavus* 21-3 consumed ZVS as nutrient and thereby generating energy to support bacterial growth.

In combination of above results, we proposed that ZVS production and secretion were energy conservation and detoxification strategies for *E. flavus* 21-3 to adapt deep-sea cold seeps. They utilized abundant thiosulfate as nutrition, converted it to ZVS. Then ZVS was transported outside of cells for avoiding accumulating high concentration of intracellular sulfur. Subsequently, as their energy reserves, *E. flavus* 21-3 attached to and utilized ZVS as the electron donor for better growth.

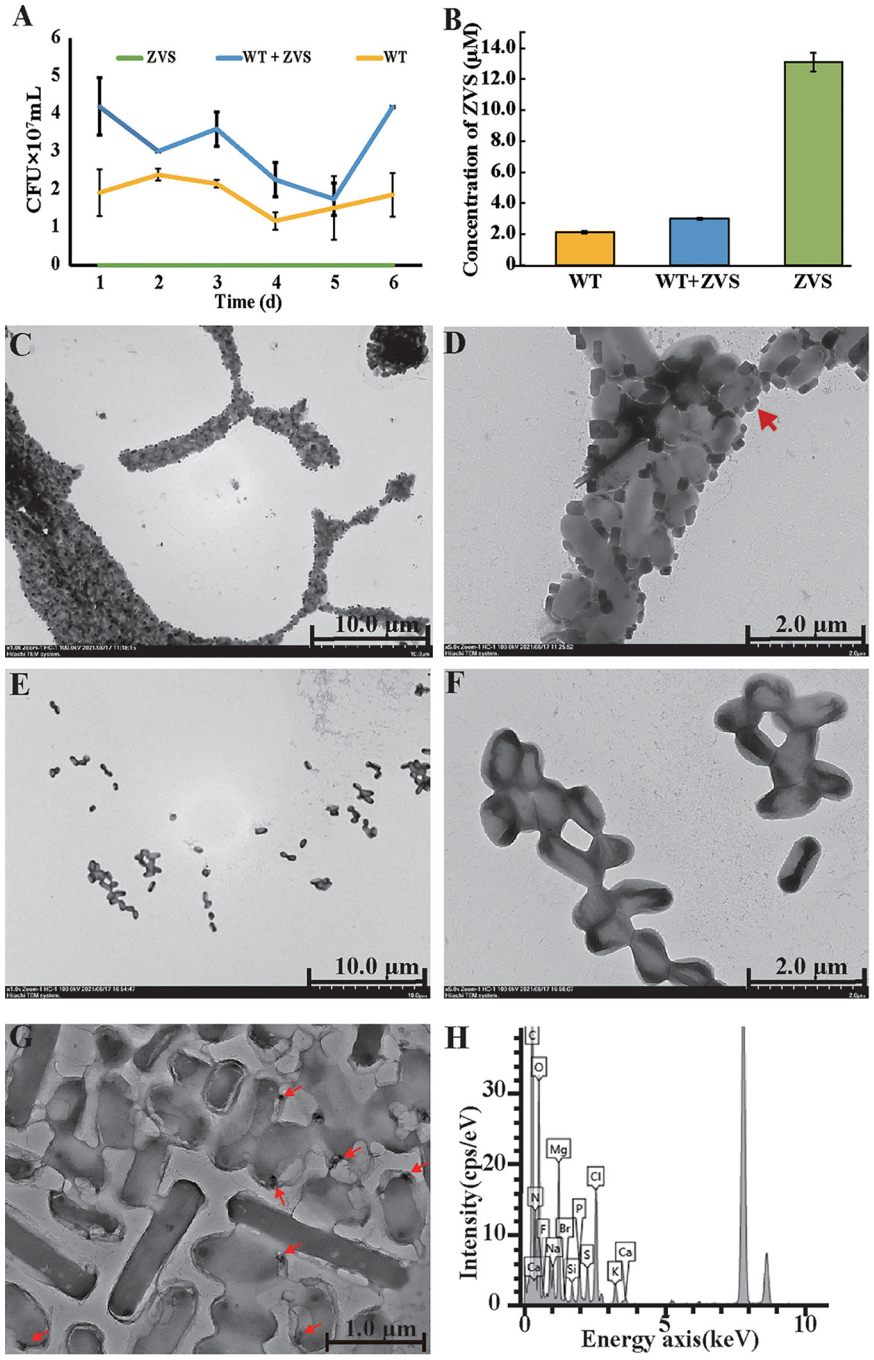

FIG 4 Assay of the effect of ZVS on the growth of *E. flavus* 21-3. (A) Growth curve of *E. flavus* 21-3 that cultivated in the medium supplemented with or without 20 mM biogenic ZVS. (B) Measurement of the concentration of ZVS in *E. flavus* 21-3 that cultured in the medium supplemented with or without 20 mM biogenic ZVS for 6 days. TEM images of *E. flavus* 21-3 that cultivated in the medium supplemented with (C, D) or without (E, F) 20 mM biogenic ZVS for 14 days. (G) TEM images of the substances formed on the surface of *E. flavus* 21-3 that cultivated in the medium supplemented with 20 mM biogenic ZVS for 14 days. (H) Energy dispersive spectrum analysis of the black particles attaching to the cell surface shown in panel G.

Comparative analyses of ZVS formation of *E. flavus* 21-3 incubated in the deep-sea cold seep and laboratory. In our previous study (6), we found that the mutant Δ*tsdA* was unable to produce ZVS in the presence of thiosulfate in the laboratorial condition due to the defect of conversion of thiosulfate to tetrathionate. However, the mutant Δ*tsdA* was able to produce a small amount of ZVS in the deep-sea cold seep

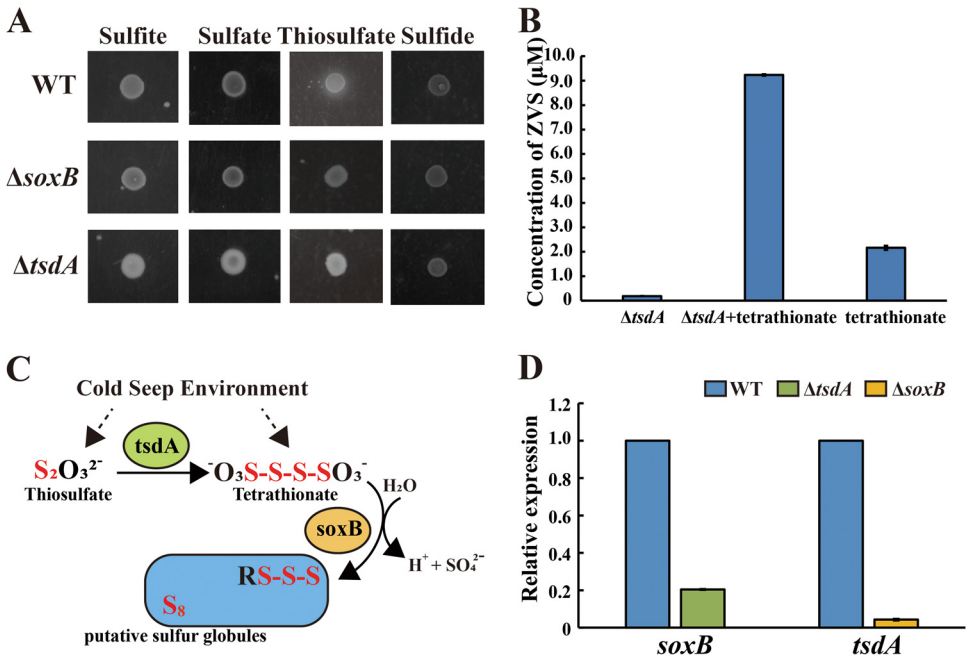

FIG 5 Tetrathionate contributes to ZVS formation of *E. flavus* 21-3 that cultured in the deep-sea cold seep. (A) Analysis of the formation of ZVS by *E. flavus* 21-3 wild type and mutants Δ*tsdA* and Δ*soxB* in the laboratorial condition in the medium supplemented with 5 mM sulfide, 40 mM sulfate, 40 mM sulfite or 20 mM thiosulfate. (B) Measurement of the yield of ZVS formed by the mutant Δ*tsdA* that cultivated in the medium supplemented with or without 10 mM tetrathionate. (C) The proposed thiosulfate oxidation pathway of *E. flavus* 21-3 cultured in the deep-sea cold seep. (D) Relative gene expression of *tsdA and soxB* in the mutants Δ*soxB* and Δ*tsdA* that cultured in the deep-sea cold seep.

(Fig. 1 and 2). Given the existence of different sulfur-containing compounds in the cold seep (Table S1 in the supplemental material), we thus asked whether the mutant Δ*tsdA* could utilize other substrates to produce ZVS. Accordingly, the mutant Δ*tsdA* was incubated in the medium supplemented with 5 mM sulfide, 40 mM sulfate, 40 mM sulfite, 20 mM thiosulfate or 10 mM tetrathionate, and ZVS was only produced in the sterile seawater added with tetrathionate (Fig. 5A and B). Therefore, we proposed that the mutant Δ*tsdA* was able to take in tetrathionate from the cold seep and thereby transferring to ZVS (Fig. 5C). To further verify this deduction, the expressions of *soxB* and *tsdA* in the WT and the mutant Δ*tsdA* or Δ*soxB* that incubated in the deep-sea cold seep were measured through qRT-PCR. Transcription of *soxB* in the mutant Δ*tsdA* could be detected, while about 5-fold lower than that in the WT (Fig. 5D). On the other hand, transcription of *tsdA* in the mutant Δ*soxB* was hardly detected (Fig. 5D). Therefore, SoxB was proposed to be functional of metabolizing tetrathionate in the mutant Δ*tsdA*. But the efficiency of ZVS production was much lower than the WT based on the yield of ZVS produced by the mutant Δ*tsdA* was less than the WT (Fig. 2E). We ever tried to determine the concentration of tetrathionate in the cold seep sediments but failed because tetrathionate was unstable in the sediments when transported and stored (7, 30). However, several reports described that tetrathionate was an important immediate of the sulfur cycle in marine sediments (31–33). Therefore, we proposed tetrathionate should exist in the deep-sea cold seep where we isolated strain 21-3 and performed *in situ* experiments. Though the formation of ZVS in the mutant Δ*tsdA* was a bit different for *in situ* and laboratorial conditions, the thiosulfate oxidation pathway determined by *tsdA* and *soxB* worked in both deep-sea and laboratorial conditions.

From above results, because of totally different conditions between laboratory and deep-sea cold seep, laboratorial study cannot truly show how bacteria work in *in situ* environment. So, to further compare the metabolism especially the thiosulfate

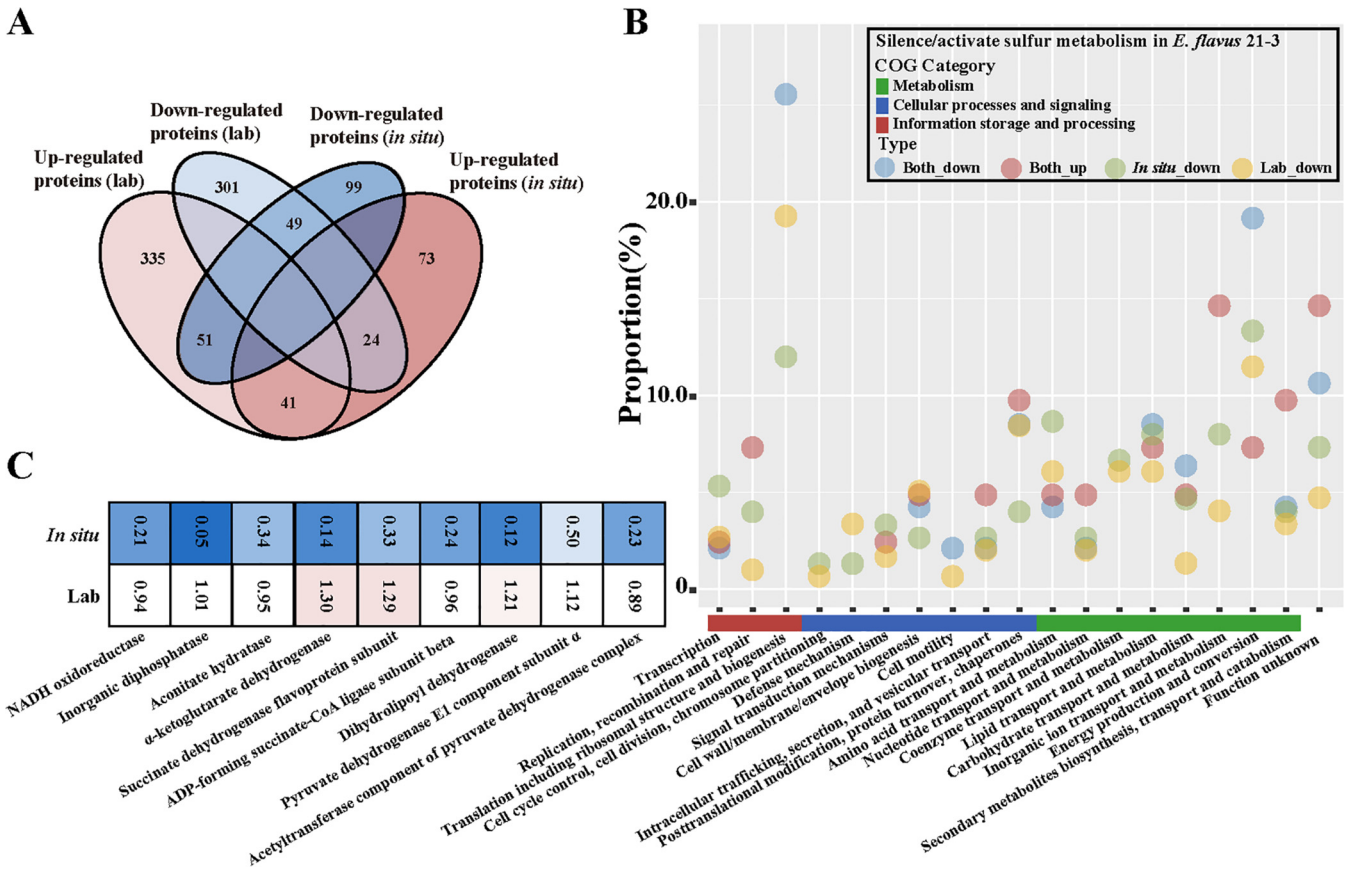

FIG 6 Comparative proteomic analysis of *E. flavus* 21-3 wild type cultivated in the laboratory or cold seep (*in situ*) when activating or silencing the thiosulfate oxidation pathway (A) Venn diagram depicting unique and shared orthologous protein clusters in each of four samples (up-regulated/down-regulated proteins in the *E. flavus* 21-3 wild type cultivated in the laboratory or deep-sea cold seep). (B) The proportion of expressed proteins in *E. flavus* 21-3 in different COG categories. The expressed proteins were indicated as proteins which were both up-regulated or both down-regulated in the laboratory and cold seeps, or were down-regulated in either of ones. (C) Heatmap analysis of differentially expressed proteins contributing to energy production and conversion of *E. flavus* 21-3 that cultivated in the laboratory and deep-sea cold seep.

oxidation pathway in *E. flavus* 21-3 incubated in the cold seep and laboratory, comparative proteomic analyses were performed. Based on results above, when *soxB* was knocked out, the thiosulfate oxidation pathway of *E. flavus* 21-3 was silenced and ZVS was absent. When we compared the protein expressions between WT and the mutant Δ*soxB* cultivated in the cold seep and laboratory respectively, big differences were found. Three hundred and one of 807 and 99 of 337 proteins were down-regulated in *E. flavus* 21-3 that incubated respectively in the laboratory and cold seep when the thiosulfate oxidation pathway was silenced (Fig. 6A). And only 49 proteins were down-regulated in both two conditions described above. The functional composition of unique and shared up-regulated/down-regulated proteins of *in situ* and laboratory groups was further analyzed based on the COG categories. The result showed that shared down-regulated proteins majorly contributed to energy production and conversion and translation including ribosome structure and biogenesis (Fig. 6B). *In situ* unique down-regulated proteins mostly belonged to energy production and conversion and contributed to energy production and conversion showed few changes in ones expressed in the laboratory (Fig. 6C). It meant that the presence of the thiosulfate oxidation pathway was more important for *in situ* incubated *E. flavus* 21-3 than those cultivated in the laboratory. Besides, in 13 of 19 COG categories, unique downregulated proteins of *in situ* incubated *E. flavus* 21-3 were more than those incubated in the laboratory, suggesting that the absence of the thiosulfate oxidation pathway impacted metabolisms of *in situ* incubated *E. flavus* 21-3 more

negatively. These results highlighted the importance of the thiosulfate oxidation pathway for *E. flavus* 21-3 to adapt deep-sea special conditions.

Broad distribution of the novel thiosulfate oxidation pathway in deep-sea cold seeps. To investigate the sulfur cycle of cold seep sediments of the study site, metagenomic analyses were performed. Sediments sampled for sequencing were collected from different depths: 0–20 cm, 20–40 cm, and 40–60 cm below the seafloor; and 2,653,537 gene sequences and 81 bacterial metagenomes sequenced from sediments were annotated based on the KEGG and Uniprot database. The result showed that the abundance of genes associated with sulfur cycle decreased with the increasing depth of sediments (Fig. 7A). Proposed sulfur cycles in the sediments of different depths were constructed based on the distribution of metagenes (Fig. 7B). Sulfur oxidation genes were decreased with increasing depth. The presence of sulfur oxidation resulted in more abundant sulfur cycling associated genes in the shallower sediments.

To further investigate the contribution of the thiosulfate oxidation pathway identified in *E. flavus* 21-3 in the cold seep, *soxB* and *tsdA* gene homologs were identified in the metagenomic data. In the 0–40 cm sediments, the metagenomes containing both *tsdA* and *soxB* homologous genes constituted ~25% of all bacteria metagenomes. In the 0–20 cm sediments, more *tsdA* and *soxB* homologous genes were identified. It meant that bacteria, which potentially possess the thiosulfate oxidation pathway identified in *E. flavus* 21-3, were mainly distributed in the shallow cold seep sediments which containing abundant sulfur cycling genes. Given the key roles of *tsdA* and *soxB* gene homologs, this pathway potentially existed in many microorganisms in the cold seep. Besides, abundant ZVS was ever found in the shallow sediments of cold seep and was regarded as important immediate in the active sulfur cycle of cold seep (1–3). Therefore, we proposed that the microbial contribution of this pathway to the formation of ZVS and the sulfur cycle in the cold seep couldn't be ignored.

MATERIALS AND METHODS

***In situ* cultivation of *E. flavus* 21-3.** *E. flavus* 21-3 WT and mutants with deletion of key gene(s) determining the formation of ZVS were cultivated in 50 mL artificial seawater (ASW) 2216E broth (0.5% tryptone, 0.1% yeast extract in 50 mL ASW) at 28°C with shaking at a speed of 150 rpm until $OD_{600} \approx 0.1$. The ASW contained: 24.47 g NaCl, 3.917 g Na_2SO_4, 0.664 g KCl, 0.024 g SrCl, 4.981 g $MgCl{\cdot}6H_2O$, 1.102 g $CaCl_2$, 0.192 g $NaHCO_3$, 0.026 g H_3BO_4, and 0.0039 g NaF per 1 L of Milli-Q water. The pH was adjusted to 7.2–7.5 using 1 M NaOH. Cells were collected by centrifugation at 1,000 × *g* for 10 min and washed three times in the ASW. Then washed cells were transferred to 50 mL ASW in the dialysis tubes which allow exchanging ions in the cold seep. Finally, strains were incubated in the cold seep of the South China Sea for 10 days using the remotely operated vehicle (ROV) of RV *KEXUE* as previously described (34). Three biological replicates were performed.

ZVS purification. One liter cultures of *E. flavus* 21-3 were cultured at 28°C in the 2216E medium with 40 mM thiosulfate for 24 h. ZVS was purified from cultures by sucrose density gradient centrifugation (28, 35). ZVS and cells were collected by centrifugation at 1,000 × *g* for 10 min at 10°C. Cells and ZVS were resuspended in 5 mL sterile 2.5 M sucrose solution ($\rho \approx 1.32$ g/mL) after removing the supernatant. The suspension was transferred into 45 mL of sterile 2.5 M sucrose solution. The ZVS was pelleted through the sucrose solution by centrifugation at 4,000 × *g* for 10 min at 10°C. The supernatant was removed and the collected ZVS was resuspended in 100 mL of sterile 2.5 M sucrose solution two more times. Collected ZVS resuspended with 50 mL sterile ASW was centrifuged at 16,200 × *g* for 5 min at 4°C. This step was repeated twice to remove sucrose. ZVS was resuspended and vortexed for several minutes to detach any remaining cells and allowed settling without centrifugation. The supernatant was removed. The latter step was repeated two more times. Then, the pellets were suspended with 75% alcohol and centrifuged at 5,000 × *g* for 10 min at 4°C. Finally, the supernatant was removed, the pellets were resuspended in sterile seawater and the suspension was stored at 4°C.

Cultivation of *E. flavus* 21-3 WT and mutants Δ*tsdA* and Δ*soxB* in the medium supplemented with sulfide, sulfate, sulfite, thiosulfate, or ZVS. To confirm whether *E. flavus* 21-3 grew better in the presence of ZVS, 20 mM purified ZVS produced by *E. flavus* 21-3 was added to 50 mL sterilized ASW to cultivate *E. flavus* 21-3 at 28°C with shaking at a speed of 150 rpm for 7 or 14 days; 50 mL ASW added 20 mM ZVS and 50 mL ASW added *E. flavus* 21-3 were set as control groups. The growth condition was determined by the plate count method. Briefly, medium was diluted gradually, spread on the 2216E medium plate and counted the number of colonies after 3-day cultivation.

To detect whether *E. flavus* 21-3 WT and mutants Δ*tsdA* and Δ*soxB* could utilize sulfide, sulfate, sulfite and thiosulfate, 2216E solid medium supplemented with 5 mM sodium sulfide, 40 mM sodium sulfate, 40 mM sodium sulfite or 20 mM sodium thiosulfate was used to cultivate *E. flavus* 21-3 WT and mutants Δ*tsdA* and Δ*soxB*.

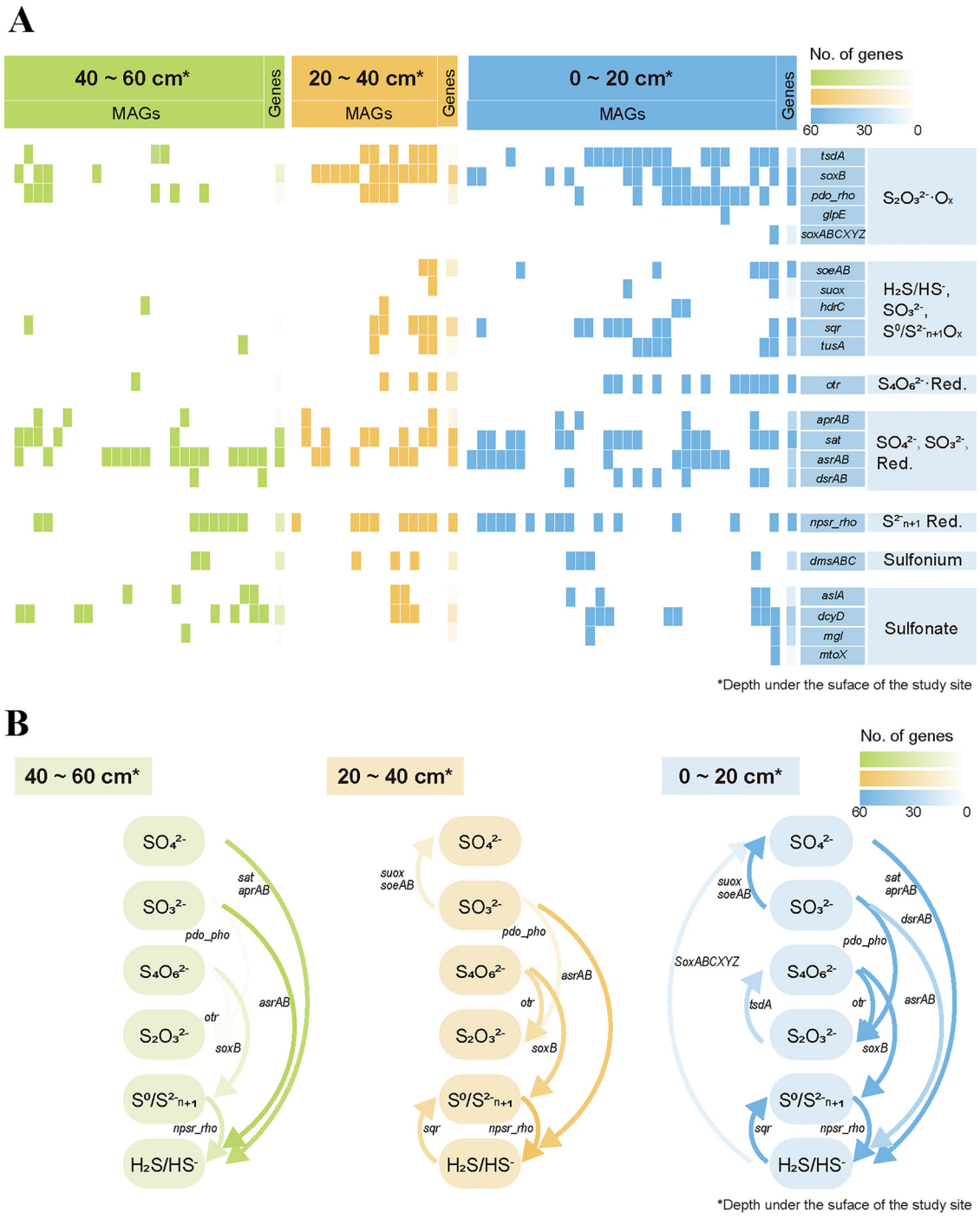

FIG 7 Metagenomic analysis of the distribution of sulfur metabolism-related genes in different depths of the study site. (A) Vertical profiles of sulfur cycling associated genes identified in metagenomes along geochemical gradients. The numbers of genes per sample were normalized. The genes used in this analysis were listed in Table S3. (B) Schematic representation of the sulfur cycle in different depths of the study site.

To detect whether *E. flavus* 21-3 mutant Δ*tsdA* transformed tetrathionate to ZVS, the mutant Δ*tsdA* was cultivated in 50 mL sterilized ASW supplemented with 10 mM sodium tetrathionate at 28°C with shaking at a speed of 150 rpm for 3 days; 50 mL sterilized ASW with 10 mM sodium tetrathionate and 50 mL sterilized ASW were set as control groups. The concentration of ZVS was determined as the method described in the following part.

Electron microscopic analyses of bacterial cells and ZVS produced by *E. flavus* 21-3 in the deep-sea cold seep. To observe the morphological characteristics of the *in situ* incubated bacteria, cells were collected by centrifugation (1,000 × *g*, 10 min, 4°C), preserved in 25% (vol/vol) glutaraldehyde overnight

at 4°C and washed three times using phosphate-buffered saline (PBS) in the next day. Later, samples were dehydrated in the ethanol solution of 30%, 50%, 70%, 90% and 100% for 10 min each time. Then samples were transferred to isoamyl acetate for 20 min at room temperature. Finally, the samples were dried by critical-point drying and coated with graphite and gold. SEM (S-3400N, Hitachi, Japan) was performed to observe samples at 5 keV. For transmission electron microscopy (TEM), *in situ* incubated strains were collected by centrifugation (1,000 $\times$ *g*, 10 min, 4°C), washed three times using PBS and dried at room temperature. TEM (HT7700; Hitachi, Japan) was used to observe samples at 100 keV. To identify the element component of cell attachments, Energy-Dispersive Spectrum (EDS) (model 550i, IXRF systems, USA) equipment with SEM was used at an accelerating voltage of 5 keV for 30 s.

To identify the ZVS produced by *E. flavus* 21-3, TEM was used to observe the morphology of ZVS firstly and Raman spectrum (WITec alpha300 R system; WITec Company, Germany) was used to identify the components and structures. After incubation with ZVS, *E. flavus* 21-3 treated as described above was observed through TEM (JEM-2100PLUS, Jeol, Japan). And EDS (X-Max 80. Oxford Instruments, UK) equipment with TEM was used at accelerating voltage to identify the element component of cell attachments.

To further observe the morphological characteristics of bacterial cells, ultrathin-section electron microscopic observation was performed as described previously (36, 37). Briefly, samples were prepared as procedures for SEM observation, and then the dehydrated samples were embedded in a plastic resin. Ultrathin sections (50–70 nm) of cells were prepared with an ultramicrotome (Leica EM UC7, Germany), stained with uranyl acetate and lead citrate. All samples were examined using TEM (HT7700, Hitachi, Japan) at 100 kV.

Analytical techniques for the determination of sulfate, sulfite, sulfide, thiosulfate and ZVS. The concentration of sulfate, sulfite and thiosulfate in the seawater and sediment of the study site was monitored by ion chromatography (ECO-IC, Shimadzu, Japan) fitted with a Shodex IC SI-52 4E column (Shodex, Japan) at a constant column temperature of 25°C. Then the column was eluted with 6.0 mM Na_2CO_3 and 2.0 mM $NaHCO_3$ with a flow of 0.7 mL/min. The concentration of sulfide in the seawater and sediment of the study was determined by iodometric determination (38). Briefly, 10 mL of sample solution (0.5 g sediments dissolved in 10 mL ultra-pure water or 10 mL seawater, all samples were filtered with a pore size of 0.22 μm) was mixed with 25 mL cadmium acetate solution to precipitate sulfide in forms of cadmium sulfide. Then precipitating cadmium sulfide was collected and mixed with 10 mL 0.1 M iodine solution and 3 mL hydrochloric acid. The mixture was titrated with 0.1 M sodium thiosulfate solution. The titration endpoint was determined by an automatic potentiometric titrator (T940, Thermo Fisher Scientific, USA) and the volume of consumed thiosulfate solution was recorded to calculate the concentration of sulfide. ZVS was extracted from the cultured medium using chloroform according to the method described previously (39, 40). Briefly, 3 mL sample was extracted three times using a total of 5 mL chloroform. The extracted chloroform was measured on a UV-Vis spectrometer (Infinite M1000 Pro; Tecan, Männedorf, Switzerland) at 270 nm.

Quantitative real-time PCR (qRT-PCR). For qRT-PCR, *in situ* incubated mutants Δ*tsdA* and Δ*soxB* of *E. flavus* 21-3 were collected by centrifugation (10,000 $\times$ *g*, 10 min, 4°C). Total RNAs from each sample were extracted using TRIzol reagent (Solarbio, China). The concentration of total RNAs was measured by Spectrophotometer (NanoPhotometer NP80, Implen, Germany). Then RNAs were reverse transcribed into cDNA using ReverTra Ace^{TM} qPCR RT Master Mix with gDNA Remover (TOYOBO, Japan). Transcriptional levels of different genes were determined by qRT-PCR using SYBR Green Realtime PCR Master Mix (TOYOBO, Japan) and the QuantStudio^{TM} 6 Flex (Thermo Fisher Scientific, USA). The condition of PCR was set as following: 95°C for 1 min, followed by 40 cycles of denaturation at 95°C for 15 s, annealing at 55°C for 15 s, and extension at 72°C for 15 s. 16S rRNA was used as an internal reference. The relative gene expression was calculated using the $2^{-\Delta\Delta Ct}$ method with each transcript signal normalized to that of 16S rRNA (41). Primers used were listed in the supplementary information (Table S2 in the supplemental material). All qRT-PCR runs were performed in three biological and three technical replicates.

Proteomic analysis. For proteomic analysis, *in situ* incubated bacterial cells were collected by centrifugation at 10,000 $\times$ *g* for 10 min at 4°C. Pellets were washed with 10 mM PBS (pH 7.4) and resuspended in the lysis buffer (8 M urea, 1% protease inhibitor). The resuspension was sonicated and the remaining debris was removed by centrifugation at 10,000 $\times$ *g* for 10 min at 4°C. The concentration of protein was determined with a BCA kit (Solarbio, China) after collecting supernatant. Detailed procedures of Trypsin digestion and LC-MS/MS analysis were described in the supplementary information (Text S1). All protein sequences were annotated using Uniprot (Release 2021_03), COG (updated in 2020), and KEGG databases (Release 99.1) (42). For comparative proteomic analyses, in the laboratorial condition, cells of *E. flavus* 21-3 cultivated in the medium supplemented with or without 40 mM sodium thiosulfate were respectively regarded as the active and silent sulfur-producing pathway; in the deep-sea *in situ* condition, *E. flavus* 21-3 WT and mutant Δ*soxB* were respectively regarded as the active and silent sulfur-producing pathway. Heatmap analysis and Venn diagram of studied proteins were completed by R packages pheatmap and VennDiagram respectively in R (v4.0.1).

Metagenomic analysis. Total DNA from 30 g sediments of each sample was extracted using Tianen Bacterial Genomic DNA Extraction Kit following the manufacturer's protocol. Subsequent steps (metagenomic sequencing, assembly and binning) were shown in the supplementary information (Text S1). Genes used for analyzing sulfur cycle referred to the following research and were listed in Table S3 in the supplemental material (43). Sequences were annotated using KEGG (Release 87.0), NR (2021-10-17), uniport (Release 2021_03) and COG (updated in 2020) using Diamond (v0.8.23) with 1e-20 e-value cutoff (44). Heatmap analyses of studied genes were completed by R packages pheatmap in R (v4.0.1).

Data deposit. The genomic information of *E. flavus* 21-3 has been uploaded to the NCBI with the accession number CP032228. The proteomics data have been uploaded to Proteome Xchange Consortium with the data set identifier PXD016502 and PXD029383.

SUPPLEMENTAL MATERIAL

Supplemental material is available online only.

TEXT S1, DOCX file, 0.03 MB.

FIG S1, DOCX file, 2 MB.

FIG S2, DOCX file, 0.4 MB.

FIG S3, DOCX file, 1.6 MB.

TABLE S1, DOCX file, 0.01 MB.

TABLE S2, DOCX file, 0.02 MB.

TABLE S3, DOCX file, 0.02 MB.

ACKNOWLEDGMENTS

We thank the Center for High Performance Computing and System Simulation of Pilot National Laboratory for Marine Science and Technology (Qingdao) and Demin Xu from the University of Science and Technology of China for their support in data analysis. This work was financially supported by the Marine S&T Fund of Shandong Province for Pilot National Laboratory for Marine Science and Technology (Qingdao) (Grant No. 2022QNLM050102-3), China Ocean Mineral Resources R&D Association Grant (Grant No. DY135-B2-14), Strategic Priority Research Program of the Chinese Academy of Sciences (Grant No. XDA22050301), Shandong Provincial Natural Science Foundation (ZR2021ZD28), Major Research Plan of the National Natural Science Foundation (Grant No. 92051107), Key Deployment Projects of Center of Ocean Mega-Science of the Chinese Academy of Sciences (Grant No. COMS2020Q04) for Chaomin Sun.

R.C. and C.S. conceived and designed the study; J.Z. offered study strains; R.L. completed *in situ* experiments in the deep-sea cold seep; R.C. conducted most of the experiments and analyses; W.H. and X.Z. performed the Raman spectra analyses; R.C. and C.S. led manuscript writing and all authors contributed to reviewing the manuscript.

We declare that we do not have any competing interests.

REFERENCES

1. White SN. 2009. Laser Raman spectroscopy as a technique for identification of seafloor hydrothermal and cold seep minerals. Chem Geol 259:240–252. https://doi.org/10.1016/j.chemgeo.2008.11.008.
2. White SN, Dunk R, Peltzer ET, Freeman J, Brewer PG. 2006. *In situ* Raman analyses of deep-sea hydrothermal and cold seep systems (Gorda Ridge and Hydrate Ridge). Geochem Geophys Geosyst 7:1–12.
3. Zhang X, Du Z, Zheng R, Luan Z, Qi F, Cheng K, Wang B, Ye W, Liu X, Lian C, Chen C, Guo J, Li Y, Yan J. 2017. Development of a new deep-sea hybrid Raman insertion probe and its application to the geochemistry of hydrothermal vent and cold seep fluids. Deep Sea Res Part I Oceanogr Res Pap 123:1–12. https://doi.org/10.1016/j.dsr.2017.02.005.
4. Osorio H, Mangold S, Denis Y, Ñancucheo I, Esparza M, Johnson DB, Bonnefoy V, Dopson M, Holmes DS. 2013. Anaerobic sulfur metabolism coupled to dissimilatory iron reduction in the extremophile *Acidithiobacillus ferrooxidans*. Appl Environ Microbiol 79:2172–2181. https://doi.org/10.1128/AEM.03057-12.
5. Jørgensen BB. 1990. A thiosulfate shunt in the sulfur cycle of marine sediments. Science 249:152–154. https://doi.org/10.1126/science.249.4965.152.
6. Zhang J, Liu R, Xi SC, Cai RN, Zhang X, Sun CM. 2020. A novel bacterial thiosulfate oxidation pathway provides a new clue about the formation of zero-valent sulfur in deep sea. ISME J 14:2261–2274. https://doi.org/10.1038/s41396-020-0684-5.
7. Fossing H. 2004. Distribution and fate of sulfur intermediates-sulfite, tetrathionate, thiosulfate, and elemental sulfur in marine sediments, p 97–166. *In* Amend JP, Edwards KJ, Lyons TW (ed), *Sulfur biogeochemistry: past and present*. Geological Society of America, McLean, VA.
8. Ghosh W, Dam B. 2009. Biochemistry and molecular biology of lithotrophic sulfur oxidation by taxonomically and ecologically diverse bacteria and archaea. FEMS Microbiol Rev 33:999–1043. https://doi.org/10.1111/j.1574-6976.2009.00187.x.
9. Friedrich CG, Rother D, Bardischewsky F, Quentmeier A, Fischer J. 2001. Oxidation of reduced inorganic sulfur compounds by bacteria: emergence of a common mechanism? Appl Environ Microbiol 67:2873–2882. https://doi.org/10.1128/AEM.67.7.2873-2882.2001.
10. Pronk J, Meulenberg R, Hazeu W, Bos P, Kuenen J. 1990. Oxidation of reduced inorganic sulphur compounds by *Acidophilic thiobacilli*. FEMS Microbiol Rev 75:293–306. https://doi.org/10.1111/j.1574-6968.1990.tb04103.x.
11. Pattaragulwanit K, Brune DC, Truper HG, Dahl C. 1998. Molecular genetic evidence for extracytoplasmic localization of sulfur globules in *Chromatium vinosum*. Arch Microbiol 169:434–444. https://doi.org/10.1007/s002030050594.
12. Dahl C, Prange A. 2006. Bacterial sulfur globules: occurrence, structure and metabolism, p 21–51. *In* Shively JM (ed), *Inclusions in prokaryotes*. Springer: Berlin.
13. Hensen D, Sperling D, Trüper HG, Brune DC, Dahl C. 2006. Thiosulphate oxidation in the phototrophic sulphur bacterium *Allochromatium vinosum*. Mol Microbiol 62:794–810. https://doi.org/10.1111/j.1365-2958.2006.05408.x.
14. Gregersen LH, Bryant DA, Frigaard NU. 2011. Mechanisms and evolution of oxidative sulfur metabolism in green sulfur bacteria. Front Microbiol 2:1–14.
15. Houghton J, Foustoukos D, Flynn T, Vetriani C, Bradley AS, Fike D. 2016. Thiosulfate oxidation by *Thiomicrospira thermophila*: metabolic flexibility in response to ambient geochemistry. Environ Microbiol 18:3057–3072. https://doi.org/10.1111/1462-2920.13232.
16. Lu WP, Kelly DP. 1988. Kinetic and energetic aspects of inorganic sulfur compound oxidation by *Thiobacillus Tepidarius*. J Gen Microbiol 134:865–876. https://doi.org/10.1099/00221287-134-4-865.

17. Kelly DP, Shergill JK, Lu WP, Wood AP. 1997. Oxidative metabolism of inorganic sulfur compounds by bacteria. Anton Leeuw Int J G 71:95–107. https://doi.org/10.1023/A:1000135707181.
18. Dam B, Mandal S, Ghosh W, Gupta SKD, Roy P. 2007. The S_4-intermediate pathway for the oxidation of thiosulfate by the chemolithoautotroph *Tetrathiobacter kashmirensis* and inhibition of tetrathionate oxidation by sulfite. Res Microbiol 158:330–338. https://doi.org/10.1016/j.resmic.2006.12.013.
19. De Jong GA, Hazeu W, Bos P, Kuenen JG. 1997. Isolation of the tetrathionate hydrolase from *Thiobacillus acidophilus*. Eur J Biochem 243:678–683. https://doi.org/10.1111/j.1432-1033.1997.00678.x.
20. Wang R, Lin JQ, Liu XM, Pang X, Zhang CJ, Yang CL, et al. 2019. Sulfur oxidation in the acidophilic autotrophic *Acidithiobacillus* spp. Front Microbiol 9:1–20.
21. Beard S, Paradela A, Albar JP, Jerez CA. 2011. Growth of *Acidithiobacillus ferrooxidans* ATCC 23270 in thiosulfate under oxygen-limiting conditions generates extracellular sulfur globules by means of a secreted tetrathionate hydrolase. Front Microbiol 2:1–10.
22. Tian RM, Zhang WP, Cai L, Wong YH, Ding W, Qian PY. 2017. Genome reduction and microbe-host interactions drive adaptation of a sulfur-oxidizing bacterium associated with a cold seep sponge. mSystems 2:1–14. https://doi.org/10.1128/mSystems.00184-16.
23. Gorlas A, Marguet E, Gill S, Geslin C, Guigner J-M, Guyot F, Forterre P. 2015. Sulfur vesicles from *Thermococcales*: A possible role in sulfur detoxifying mechanisms. Biochimie 118:356–364. https://doi.org/10.1016/j.biochi.2015.07.026.
24. Eichinger I, Schmitz-Esser S, Schmid M, Fisher CR, Bright M. 2014. Symbiont-driven sulfur crystal formation in a thiotrophic symbiosis from deep-sea hydrocarbon seeps. Environ Microbiol Rep 6:364–372. https://doi.org/10.1111/1758-2229.12149.
25. Maki JS. 2013. Bacterial intracellular sulfur globules: structure and function. J Mol Microbiol Biotechnol 23:270–280. https://doi.org/10.1159/000351335.
26. Franz B, Lichtenberg H, Hormes J, Modrow H, Dahl C, Prange A. 2007. Utilization of solid "elemental" sulfur by the phototrophic purple sulfur bacterium *Allochromatium vinosum*: a sulfur K-edge X-ray absorption spectroscopy study. Microbiology (Reading) 153:1268–1274. https://doi.org/10.1099/mic.0.2006/003954-0.
27. Prange A, Engelhardt H, Truper HG, Dahl C. 2004. The role of the sulfur globule proteins of Allochromatium vinosum: mutagenesis of the sulfur globule protein genes and expression studies by real-time RT-PCR. Arch Microbiol 182:165–174. https://doi.org/10.1007/s00203-004-0683-3.
28. Hanson TE, Bonsu E, Tuerk A, Marnocha CL, Powell DH, Chan CS. 2016. *Chlorobaculum tepidum* growth on biogenic S(0) as the sole photosynthetic electron donor. Environ Microbiol 18:2856–2867. https://doi.org/10.1111/1462-2920.12995.
29. Marnocha CL, Sabanayagam CR, Modla S, Powell DH, Henri PA, Steele AS, et al. 2019. Insights into the mineralogy and surface chemistry of extracellular biogenic S^0 globules produced by *Chlorobaculum tepidum*. Front Microbiol 10:1–11.
30. Kamyshny A, Jr, Ferdelman TG. 2010. Dynamics of zero-valent sulfur species including polysulfides at seep sites on intertidal sand flats (Wadden Sea, North Sea). Mar Chem 121:17–26. https://doi.org/10.1016/j.marchem.2010.03.001.
31. Mandal S, Bhattacharya S, Roy C, Rameez MJ, Sarkar J, Mapder T, Fernandes S, Peketi A, Mazumdar A, Ghosh W. 2020. Cryptic roles of tetrathionate in the sulfur cycle of marine sediments: microbial drivers and indicators. Biogeosciences 17:4611–4631. https://doi.org/10.5194/bg-17-4611-2020.
32. Jorgensen BB, Findlay AJ, Pellerin A. 2019. The biogeochemical sulfur cycle of marine sediments. Front Microbiol 10:1–27.
33. Wasmund K, Mußmann M, Loy A. 2017. The life sulfuric: microbial ecology of sulfur cycling in marine sediments. Environ Microbiol Rep 9:323–344. https://doi.org/10.1111/1758-2229.12538.
34. Zheng RK, Liu R, Shan YQ, Cai RN, Liu G, Sun CM. 2021. Characterization of the first cultured free-living representative of *Candidatus* Izemoplasma uncovers its unique biology. ISME J 15:2676–2691. https://doi.org/10.1038/s41396-021-00961-7.
35. Donà C. 2011. Mobilization of sulfur by green sulfur bacteria: physiological and molecular studies on *Chlorobaculum parvum* DSM 263. PhD thesis. Universität Bremen, Bremen, Germany.
36. Sekiguchi Y, Yamada T, Hanada S, Ohashi A, Harada H, Kamagata Y. 2003. *Anaerolinea thermophila* gen. nov., sp nov and *Caldilinea aerophila* gen. nov., sp nov., novel filamentous thermophiles that represent a previously uncultured lineage of the domain *Bacteria* at the subphylum level. Int J Syst Evol Microbiol 53:1843–1851. https://doi.org/10.1099/ijs.0.02699-0.
37. Graham L, Orenstein JM. 2007. Processing tissue and cells for transmission electron microscopy in diagnostic pathology and research. Nat Protoc 2:2439–2450. https://doi.org/10.1038/nprot.2007.304.
38. Bamesberger WL, Adams DF. 1969. Improvements in the collection of hydrogen sulfide in cadmium hydroxide suspension. Environ Sci Technol 3:258–261. https://doi.org/10.1021/es60026a001.
39. Boulegue J. 1978. Solubility of elemental sulfur in water at 298-K. Phosphorus Sulfur Silicon Relat Elem 5:127–128. https://doi.org/10.1080/03086647808069875.
40. Gagnon C, Mucci A, Pelletier E. 1996. Vertical distribution of dissolved sulphur species in coastal marine sediments. Mar Chem 52:195–209. https://doi.org/10.1016/0304-4203(95)00099-2.
41. Livak KJ, Schmittgen TD. 2001. Analysis of relative gene expression data using real-time quantitative PCR and the $2^{-\Delta\Delta CT}$ method. Methods 25:402–408. https://doi.org/10.1006/meth.2001.1262.
42. Kanehisa M, Sato Y, Morishima K. 2016. BlastKOALA and GhostKOALA: KEGG tools for functional characterization of genome and metagenome sequences. J Mol Biol 428:726–731. https://doi.org/10.1016/j.jmb.2015.11.006.
43. Vigneron A, Cruaud P, Culley AI, Couture RM, Lovejoy C, Vincent WF. 2021. Genomic evidence for sulfur intermediates as new biogeochemical hubs in a model aquatic microbial ecosystem. Microbiome 9:1–14. https://doi.org/10.1186/s40168-021-00999-x.
44. Buchfink B, Xie C, Huson DH. 2015. Fast and sensitive protein alignment using DIAMOND. Nat Methods 12:59–60. https://doi.org/10.1038/nmeth.3176.